1

The solar atmosphere

1.1   Introduction

The solar atmosphere may be broadly defined as that part of the Sun extending outwards from a level known as the photosphere where energy generated at the Sun's core begins to escape into space as radiation. Regions progressively deeper than this level are characterized by increasing densities where there are continual interactions between atoms or ions and radiation. None of this radiation escapes into space. Such regions constitute the solar interior. The photosphere can loosely be regarded as the Sun's surface, though more precisely it is a thin layer. The base of the photosphere depends on the wavelength of the radiation. A common but arbitrary definition is where the *optical depth* τ, i.e. the integral of the absorption coefficient over path length, is unity for radiation of wavelength 5000 Å (corresponding to the green part of the visible spectrum), written $\tau_{5000} = 1$. We will give further definitions of these concepts in Chapter 2. The temperature of the $\tau_{5000} = 1$ level is approximately 6400 K. Much of the absorption of visible and infrared radiation, which makes up the bulk of the Sun's radiant energy escaping from the photosphere, is due to the negative hydrogen ion H^-. The absorption of photons of radiation $h\nu$ occurs by reactions like $h\nu + H^- \rightarrow H + e^-$, i.e. the breakup of the H^- ion to form a hydrogen atom and a free electron. At sufficiently high densities, the reverse reaction ensures the replenishment of H^- ions. The rapid fall-off of total density proceeding outwards from the Sun leads to a depletion of H^- ions, and thus a decrease in absorption coefficient and optical depth. The consequence of this is that the Sun appears to have a very sharp edge at optical wavelengths.

Energy is generated in the Sun's core by nuclear reactions, in particular fusion of four protons to form ^{4}He nuclei. The energy is transferred to the rest of the solar interior by radiation out to $0.667R_\odot$ where $R_\odot = 696\,000$ km is the solar radius, i.e. radius of the photosphere, and by convection from $0.667R_\odot$ to the photosphere. By the First Law of Thermodynamics, the temperature continuously falls with distance from the energy-generating region at the Sun's core. This fall-off of temperature would be expected to continue in the solar atmosphere, starting from the base of the photosphere where $\tau_{5000} = 1$. In fact the temperature rises, eventually reaching extremely large values, giving rise to an atmosphere that emits radiation at extreme ultraviolet and X-ray wavelengths. The nature of this emission, and what can be learned from it, are the subject matter of this book.

1

2   *The solar atmosphere*

1.2   Chromosphere, transition region, and corona

Model solar atmospheres are a guide to the way in which temperature varies with height and help to provide definitions of atmospheric regions. In the well-known VAL models (Vernazza *et al.* (1981)), an initial temperature vs. height plot is used to calculate using radiative transfer equations of the emergent spectrum which is then compared with observed spectra, and adjustments to the initial temperature distribution made. According to their Model C (average solar atmosphere), there is a fall-off of temperature from the $\tau_{5000} = 1$ level, reaching $\sim$4400 K at a height of about 500 km above $\tau_{5000} = 1$, the temperature minimum level. Above the temperature minimum, the temperature rises to form a broad plateau at $\sim$6000 K, over a height range of approximately 1000–2000 km, then rises sharply. To account for large radiation losses due to hydrogen Ly-α emission, the VAL models require a small plateau at $\sim$20 000 K on the sharp temperature rise. According to the model by Gabriel (1976), this rise continues on to temperatures of 1.4×10^6 K or more. For many authors, the solar *chromosphere* is defined to be the region from the temperature minimum up to where the temperature is approximately 20 000 K. The region of the solar atmosphere where the temperature reaches $\sim$10^6 K and where the densities are very low compared with the chromosphere is the solar *corona*. A further region having temperatures of $\sim$10^5 K known as the *transition region* is in solar atmospheric models a thin layer separating the dense, cool chromosphere and tenuous, hot corona. Figure 1.1 shows (solid curve) the
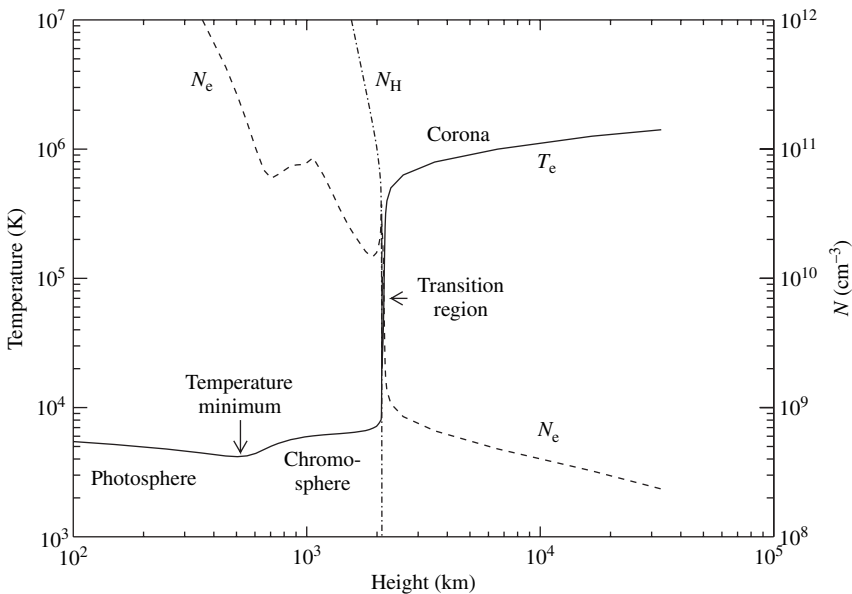

Fig. 1.1. The variation of temperature with height in the solar atmosphere (solid curve), based on one-dimensional model calculations of Vernazza *et al.* (1981), Fontenla *et al.* (1988), and Gabriel (1976). The chromospheric and transition region part of this model atmosphere is for the average quiet Sun. Based on these idealized representations of the solar atmosphere, the transition region is a thin layer with $T = 10^5$ K separating the chromosphere and corona. Variations in the number densities (cm^{-3}) of neutral hydrogen atoms (N_H) and electrons (N_e) (dot–dash and dash curves respectively) are also shown.

variation of temperature in the lower part of the solar atmosphere (heights up to 30 000 km above the $\tau_{5000} = 1$ level), together with variations in the number densities (cm^{-3}) of neutral hydrogen atoms (N_H) and free electrons (N_e), according to three quiet Sun models (Vernazza *et al.* (1981); Fontenla *et al.* (1990); Gabriel (1976)) which have been patched together over appropriate height ranges. Further details are given in Section 1.7 and Table 1.1.

The solar chromosphere is observable in visible wavelengths by forming images, known as spectroheliograms, in narrow wavelength bands around the cores of certain absorption or Fraunhofer lines that have their origins in the lower chromosphere. These include the hydrogen Balmer-α (or Hα) line at 6563 Å (red part of spectrum) and singly ionized calcium (Ca II) H and K lines at 3968 Å and 3933 Å (blue) respectively. The chromosphere also has a visible-wavelength emission-line spectrum, which is apparent at the beginning and end of the totality phase of total solar eclipses, when the Moon passes in front of the photosphere, covering up its intensely bright radiation. It is then clear that the chromosphere's extent is far greater than the 2000 km predicted by solar models and indeed its nature is far from being a uniform layer of the atmosphere. Rather, extending out from about 2000 km up to 10 000 km are transient pencil-shaped structures called spicules. In Hα spectroheliograms, they are dark features on the disk covering about 10% of the solar surface. Further, the white-light corona seen during total eclipses is observed to be highly non-uniform, consisting of streamers and loops that stretch out hundreds of thousands of kilometres above the limb. The white-light emission arises from the Thomson scattering of photospheric light by the fast-moving free electrons in the high-temperature corona. Observations, therefore, show that model atmospheres, while useful in describing the way in which temperature rises (and density decreases) with height, have limitations in that the high degree of structure in the chromosphere and corona is not properly reproduced. The nature of the transition region, predicted to be a thin layer separating the chromosphere and corona in models, may also be quite different in reality.

The bulk of the electromagnetic radiation from the chromosphere and corona has much higher photon energies than those of visible-wavelength radiation, which range from 1.6 eV to 3 eV. The characteristic radiation emitted by material with temperatures of between 10^5 K and a few MK has photon energies between 10 eV and a few 100 eV, corresponding to wavelengths between $\sim$1000 Å and less than $\sim$100 Å. The solar chromosphere and corona are therefore strong emitters of radiation with wavelengths between the ultraviolet and soft X-ray range.

The high temperatures of the chromosphere and corona, much exceeding the photospheric temperature, are plainly departures from those expected from physical considerations. A heating mechanism, due to some non-radiant energy source, is therefore required. This energy source, as well as the structured nature of the chromosphere and corona, is strongly correlated with the Sun's magnetic field, a fact that is readily observed: regions of the solar atmosphere hotter than their surroundings, as deduced from their ultraviolet and X-ray spectra, are highly correlated with regions in the photosphere associated with strong magnetic fields.

Below the photosphere, interaction between the atoms or ions and the radiation that they emit is complete, and thermodynamic equilibrium occurs. Towards the solar surface, some of this radiation begins to escape to space, and thus becomes visible to instruments on Earth. Analysis of the spectrum of this radiation shows that there is a local thermodynamic equilibrium (LTE), in which the emitted radiation is characterized by local values of temperature and density. Further out, there is an increasing departure from LTE, with the radiated energy from the photosphere interacting less and less with the surrounding material. Eventually,

ions and electrons making up the hot corona, even though bathed in the strong photospheric radiation, are nearly unaffected by it.

The Sun is a second-generation star, formed by the coalescence of material left by first-generation stars in our Galaxy that underwent supernova explosions. This is reflected in the Sun's chemical composition, which is (by number of atoms) 90% hydrogen, nearly 10% helium, with trace amounts of heavier elements. In the chromosphere, with temperatures up to 10^4 K, the hydrogen is partially ionized, so that there are large numbers of free protons and electrons as well as neutral atoms of H and He. In the corona, the ionization of both hydrogen and helium is almost complete, so that the composition is free protons and electrons and He nuclei, with much smaller numbers of ions, including those of heavier elements. Thus, the corona is for many practical purposes a fully ionized plasma, having the associated properties that we discuss in Section 1.7.

1.3   The ultraviolet and X-ray spectrum of the solar atmosphere

The comparatively high temperatures and low densities of the solar atmosphere beyond the temperature minimum region result in a spectrum in the X-ray and ultraviolet ranges which at wavelengths less than ~1400 Å is made up of emission lines and continua. The lines and continua are due to specific ions or neutral atoms, which we will indicate by the appropriate element symbol and its degree of ionization. We use throughout this book a standard spectroscopic notation identifying the ionization degree with a roman numeral; thus C I indicates the spectrum of neutral carbon (read as 'the first spectrum of carbon'), C II indicates the spectrum of once-ionized carbon ions (C^+) ('the second spectrum of carbon'), and so on. The ions themselves are indicated by superscripted numbers showing the numbers of electrons removed, e.g. C^{+3} indicates three-times-ionized carbon, which emits the C IV spectrum.

Figure 1.2 (first panel) shows the ultraviolet disk spectrum of the quiet Sun in the range 800–1500 Å from the Solar Ultraviolet Measurements of the Emitted Radiation (SUMER) instrument on the *Solar and Heliospheric Observatory* (*SOHO*). On the logarithmic flux scale of this figure, the most striking feature is the presence of recombination edges in the continuum spectrum. In the range included, these are at 912 Å (the Lyman continuum edge, due to the recombination of hydrogen), 1101 Å (recombination to neutral carbon, C I), and 1197 Å (S I). At longer wavelengths, there are edges at 1527 Å (Si I), 1683 Å (Si I), 1700 Å (Fe I), and 1950 Å (Si I). Model atmosphere calculations, such as the Harvard Smithsonian Reference Atmosphere (Gingerich *et al.* (1971)) with subsequent corrections for line blanketing and absorption by molecules, give information about the location in the quiet Sun atmosphere where these continuum sources arise. Broadly, the continuum at wavelengths above the Si I edge at 1683 Å is emitted at photospheric layers, the region between the two Si I edges at 1527 Å and 1683 Å is emitted in the temperature minimum region, and the continuum shortward of 1527 Å is chromospheric in origin. Like the visible photospheric spectrum, spectroheliograms made in the ultraviolet continuum at $\lambda > 1683$ Å show limb darkening. Immediately below this wavelength, and continuing into the X-ray range, spectroheliograms in the continuum emission show limb brightening.

To the long-wavelength side of each recombination edge are members of line series that converge on each edge. Thus, members of the hydrogen Lyman line series converge on the Lyman continuum edge at 912 Å. The most prominent member of this series, and indeed the most intense (by two orders of magnitude) line of the entire solar ultraviolet spectrum, is the Ly-α line at 1215.67 Å. As this line can normally only be emitted in regions cool enough for
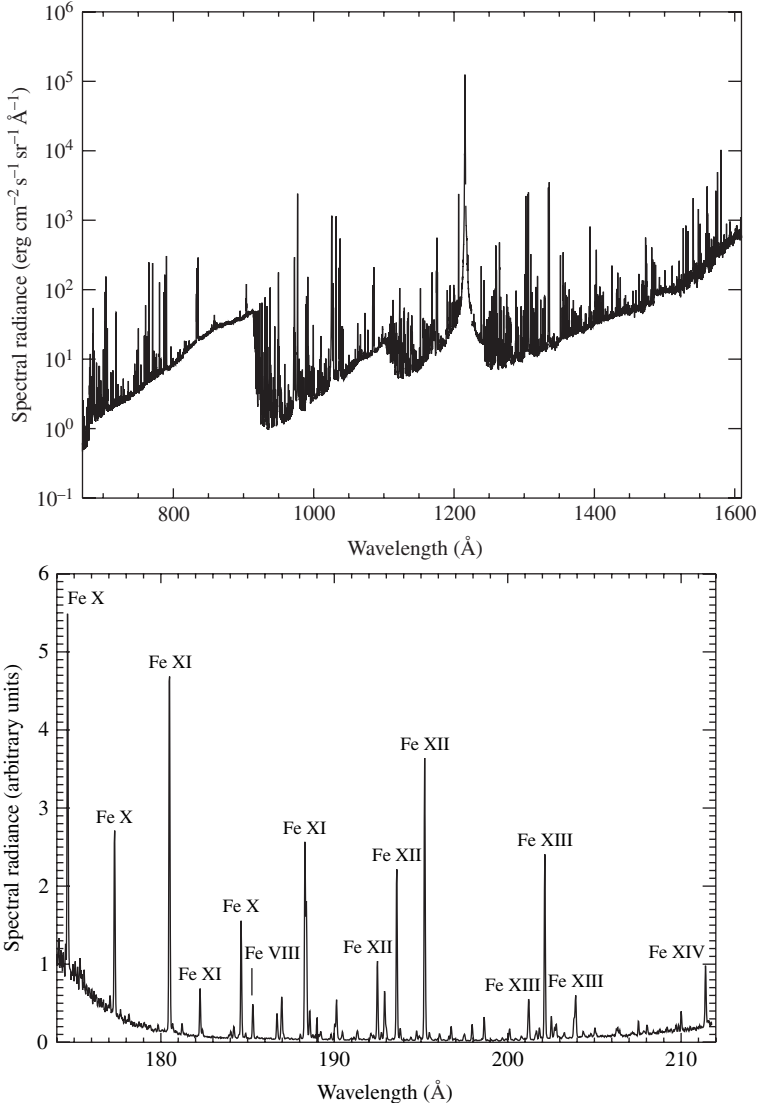
Fig. 1.2. Examples of solar ultraviolet, extreme ultraviolet, and X-ray spectra. (*First*) *SOHO* SUMER quiet Sun disk spectrum in the 675–1600 Å range, showing the Lyman lines (particularly Ly-α line at 1215.67 Å), the Lyman recombination edge at 911.8 Å and the C I recombination edge at 1101.2 Å. Courtesy *SOHO* SUMER team. (*Second*) Quiet Sun disk spectrum from the Extreme-ultraviolet Imaging Spectrometer (EIS) on the *Hinode* spacecraft, showing the diagnostically important lines of Fe ions between 174 Å and 212 Å, formed at coronal temperatures. Courtesy the *Hinode* EIS Team. (*Third*) Flare X-ray spectrum from the Flat Crystal Spectrometer on *Solar Maximum Mission*.
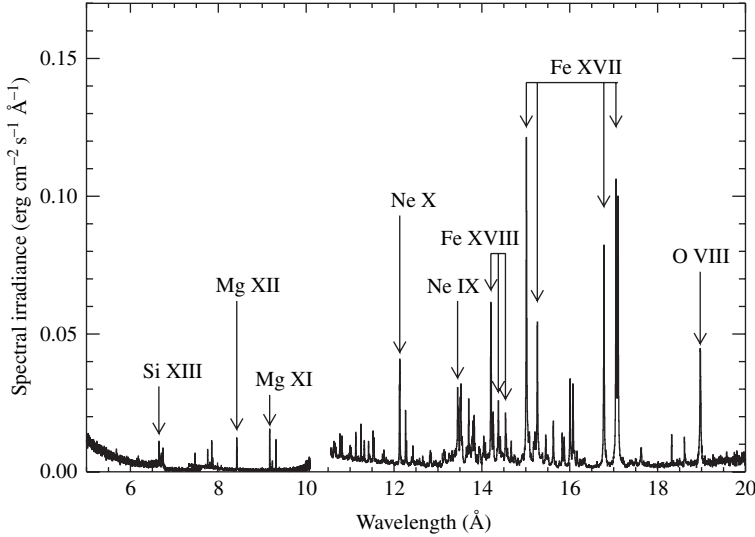
neutral hydrogen to exist, its emission has its origins almost entirely in the chromosphere, though Ly-α emission by recombination and resonant scattering has been observed in the high-temperature corona (Gabriel *et al.* (1971)). The high abundance of hydrogen results

6 *The solar atmosphere*

Fig. 1.2. *continued.*

in the line core being optically thick, and the line profile has a double reversal. There are two emission peaks separated by about 0.4 Å, with an absorption core that is formed high in the chromosphere, where the temperature is 40 000 K. The total width (FWHM) of the line is 0.7 Å, but the wings of the line, formed in the low chromosphere (temperature 6000 K), extend out to about 15 Å either side of the line core. The amount of the absorption dips in the line profile centre varies according to the solar feature emitting the Ly-α line – see Figure 1.3, based on measurements of Fontenla *et al.* (1988). Actually, the Ly-α line is in theory a doublet through the interaction of the spin of the single electron in hydrogen with the orbital angular momentum of the electron, but the separation of the two components (0.0054 Å) is far less than the width of the solar line profile, which is determined by Doppler (thermal velocity) and Stark (pressure) mechanisms as well as instrumental broadening (this is about 0.01 Å for the measurements shown in Figure 1.3). Other prominent lines in the Lyman series include Ly-β (1025.72 Å, also doubly reversed), Ly-γ (972.54 Å), and Ly-δ (949.74 Å). Helium emission lines are also prominent, those due to both neutral (He I) and ionized (He II) atoms. Since ionized helium is like hydrogen but with a nuclear charge of +2 instead of +1 atomic units, its spectrum consists of a sequence of Lyman-like spectral lines but with wavelengths that are a factor 4 smaller than those of H. The Ly-α line of He II is thus a prominent line at 303.79 Å, formed in the transition region. Neutral helium lines have a rather more complex sequence, with lines at 584.33 Å, 537.03 Å, 522.21 Å etc., all chromospherically formed.

Thousands of other emission lines occur in the 675–1600 Å quiet Sun spectrum (Figure 1.2, first panel), emitted in the chromosphere, transition region, and corona by ions of elements other than H or He. In the Appendix, we give a comprehensive list of these lines with wavelengths and identifications. The most intense emission lines are generally emitted by ions of abundant elements such as C, N, O, Ne, Mg, Si, S, Ar, Ca, and Fe. Broad groups of strong lines may be identified, such as the resonance lines of particular ions of different
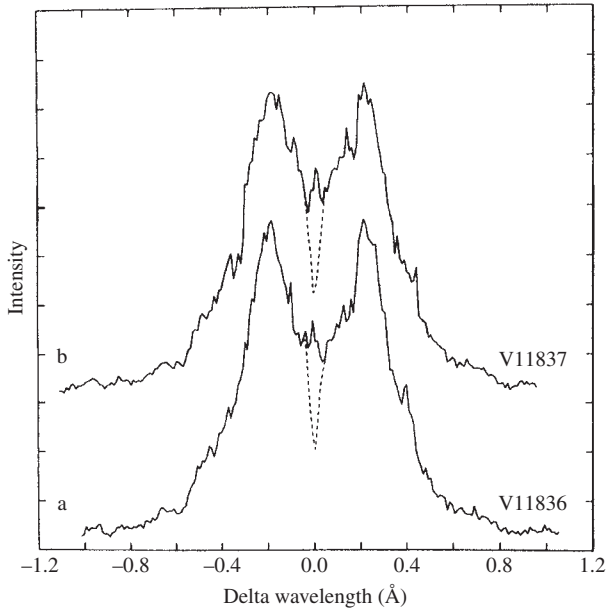
Fig. 1.3. Two examples of averaged quiet Sun Ly-α line profiles obtained by the Ultraviolet Spectrometer and Polarimeter on the *Solar Maximum Mission* spacecraft (the numbers on the plots are serial numbers of exposures from this instrument). The dashed curves are the raw data which are corrected (solid curve) for absorption by the geocorona. From Fontenla *et al.* (1988).

elements with common electron configurations. To define these spectral lines, we use a spectroscopic notation that describes both the atomic states and the transitions between them giving rise to the emission lines. We will use this notation here, but defer a full description to Chapter 3. Prominent among these lines are the resonance lines of Li-like ions, for which the transitions are $1s^2\, 2s\,{}^2S_{1/2} - 1s^2\, 2p\,{}^2P_{1/2,3/2}$. Because of the two possible orientations of the spin of the $2p$ electron in the excited state, the resonance lines are all doublets, with the lines having 2:1 flux ratios. The resonance lines in Li-like C (C IV) occur at 1548.20, 1550.77 Å, and are emitted at transition region temperatures (10^5 K). Similarly, the equivalent Li-like N (N V) lines are at 1238.82, 1242.80 Å. The Li-like O (O VI) lines (1031.91, 1037.61 Å) and Li-like Mg (Mg X) lines (609.80, 624.95 Å) have their origins in the corona (temperatures ~1 MK). The separation of the doublet lines increases markedly with atomic number.

At shorter wavelengths the many prominent emission lines again include those originating in the chromosphere, transition region, and corona, up to temperatures of 2 MK. Figure 1.2 (second panel) shows a quiet Sun spectrum from the Extreme-ultraviolet Imaging Spectrometer (EIS) on the Japanese *Hinode* spacecraft, launched in 2006. The spectrum includes resonance lines of a range of Fe ions, from Fe VIII (formed at a little less than 1 MK) to Fe XIV (~2 MK). These strong lines arise from transitions involving electrons in the $n = 3$ shell. The Fe X line at 174.53 Å, emitted at 1 MK, and an Fe IX line at 171.07 Å (not shown in the figure), though always weak in Hinode EIS spectra because of the small effective area in this region, are important emission contributors to the so-called 171 Å filters of the *SOHO* Extreme-ultraviolet Imaging Telescope (EIT) and the *Transition Region And Coronal*

Explorer (*TRACE*) imaging instruments, which we will refer to frequently throughout this book. Nearby Fe XII lines, notably that at 195.12 Å, are emitted at a slightly higher temperature, 1.4 MK, and are the most important contributors to the EIT and *TRACE* 195 Å filters for the non-flaring Sun. In the quiet Sun spectrum shown in the figure, the principal lines of Fe X, Fe XI, and Fe XII are comparable to each other in flux, indicating an average temperature of 1.2 MK for the emitting region. At higher wavelengths, not included in this quiet Sun spectrum, is the strong Fe XV line at 284.16 Å, emitted at 3 MK, which is the only strong line within the range of the 284 Å EIT and *TRACE* filters.

At X-ray wavelengths, emission lines due to other highly ionized species exist, but are only strong when emitted by intense active regions on the Sun or more particularly solar flares. The ions emitting the lines are often those that have filled outer shells, such as the neon-like (electron configuration $1s^2\,2s^2\,2p^6$, i.e. $n = 2$ shell filled) or helium-like stages ($1s^2$, i.e. $n = 1$ shell filled). Thus, strong emission lines due to neon-like Fe (Fe XVII) occur at 15.01 Å, 16.78 Å, 17.05 Å, and 17.10 Å. Other strong lines include those due to helium-like C (C V) at 40.27 Å and helium-like O (O VII) at 21.60 Å. Such lines can be emitted by quiet coronal structures, with temperatures of about 1–2 MK, but become much more intense when emitted by active regions or flares, for which the temperatures are much higher still (Section 1.6). Figure 1.2 (third panel) shows the X-ray spectrum emitted by a hot flare plasma in its decaying phase observed with the *Solar Maximum Mission* Flat Crystal Spectrometer, a Bragg diffracting crystal spectrometer with several crystals covering a range extending from 1.4 Å to 22.4 Å. The Ly-α lines of H-like O (O VIII, 18.97 Å), Ne (Ne X, 12.13 Å), and Mg (Mg XII, 8.42 Å) are all prominent. Lines due to transitions between the $n = 2$ and $n = 3$ shells of Ne-like Fe (Fe XVII) are the most intense in this range, but there are also similar transitions in F-like Fe (Fe XVIII).

At the peak of strong flares, the hot plasma, with temperatures of 15–30 MK, is characterized by Fe ions in higher stages of ionization, up to the He-like (Fe XXV) or even H-like (Fe XXVI). Such ions need temperatures of ∼20 MK and ∼30 MK for their formation. The resonance line of Fe XXV, due to $1s^2 - 1s2p$ transitions, is at 1.85 Å, and is a prominent feature of X-ray spectra detected by crystal spectrometers on solar spacecraft missions dedicated to the study of flares. These include the US Air Force *P78-1* spacecraft, the NASA *Solar Maximum Mission* that flew in the 1980s, and the more recent *Reuven Ramaty High-Energy Solar Spectroscopic Imager* (*RHESSI*) with broad-band spectral resolution, having a range that extends downwards from ∼4 Å (or in terms of equivalent photon energy units, energies above 3 keV). Throughout the entire X-ray range, and indeed throughout the EUV range, there is a continuum, emitted by free–free and free–bound processes. Relative to the lines, which become rather sparse in the higher-energy X-ray range, the continuum makes a larger contribution to the total emission. Also of increasing importance for X-ray line emission is the presence of *dielectronic* lines, formed by dielectronic recombination processes. An electron may recombine with an ion in a coronal plasma by a radiative process, in which the excess energy of the electron is removed from the atom by a photon of arbitrary energy, hence the formation of free–bound, or recombination, continuous emission. But resonance recombination processes also occur, in which an electron with a precisely defined energy recombines with an ion to produce a doubly excited ion, i.e. with two electrons instead of the normal one in excited shells. If one of these electrons de-excites, the resulting photon contributes to a dielectronic satellite line, so-called because the line generally accompanies

a parent resonance line on the long-wavelength side. Such satellites are frequently an important way of diagnosing the flare plasma, giving information on its temperature in particular. This is discussed in Chapter 5.

1.4   Structure of the solar atmosphere

An important characteristic of the solar photosphere, which has consequences for the solar atmosphere, is convection. Convection occurs on large scales in the outer parts ($>0.667R_\odot$) of the solar interior, where it dominates over radiation as the energy transfer process. Near the solar surface, a small-scale convection pattern consisting of cell structures or *granules* occurs, with typical sizes of $\sim$100–1100 km and lifetimes of several minutes. Granules are visible in white-light images of the photosphere as slightly brighter areas with polygonal shapes that are characteristic of surface convection cells formed in the laboratory. Of more importance for our purposes are the *supergranules*, recognizable from the Doppler shifts of photospherically formed Fraunhofer lines. Material from the interior is convected upwards at the cell centre, then radially outwards and nearly horizontally with velocities of 0.4 km s^{-1} towards the cell boundaries, where it is convected downwards with velocities of about 0.1 km s^{-1}. Supergranules are thought to be pancake-like structures, approximately 30 000 km across and a few thousand km thick, and lasting from one to several days.

Spectroheliograms formed at the wavelengths of certain weak Fraunhofer lines, particularly the so-called G band (actually a band-head in the solar spectrum, at 4290–4310 Å, due to the CH molecule), show filigree-like strings of fine bright points, about 100 km across, in the dark lanes between granules. A pattern or network of bright points is recognizable, coincident with the supergranule boundaries. The bright points are associated with strong ($\sim$1000 G) magnetic field, probably in the form of magnetic flux tubes emerging from below the photosphere. The supergranular convective flow transports material and also concentrations of magnetic field towards the supergranule boundaries, so a network of magnetic field is formed, corresponding to the network of bright points. This field, with strengths of several hundred gauss, is detectable using the Zeeman effect, with magnetically sensitive absorption lines at visible wavelengths. The Michelson Doppler Imager (MDI) on *SOHO* routinely measures the line-of-sight component of the field, producing full Sun magnetograms such as those shown in Figure 1.4. The field may be positive (field lines directed towards the observer, or outwards from the Sun) or negative (field lines away from the observer, or towards the Sun), and exists all over the Sun's surface. (At the time of writing, the spectro-polarimeter part of the Solar Optical Telescope (SOT) on board the Japanese *Hinode* spacecraft is obtaining field strength and direction information, producing vector magnetic field maps.)

Magnetic field clumps at the photospheric level are associated with enhanced heating in the solar atmosphere, with consequent increased brightening at certain wavelengths in chromospheric and coronal features where the field is concentrated. The pattern of magnetic field concentrations in the quiet Sun results in a corresponding pattern of emission features formed in the chromosphere and transition region known as the quiet Sun chromospheric network. In visible wavelengths, the pattern can be seen in the Hα and ionized calcium (Ca II) H and K absorption lines. The cores of these lines are formed in the low chromosphere. In the Hα line, the network takes the form of groups of spicules or pencil-shaped features pointing out approximately radially from the photosphere. In the Ca II lines, the network (sometimes called the calcium network) consists of bright structures roughly delineating the
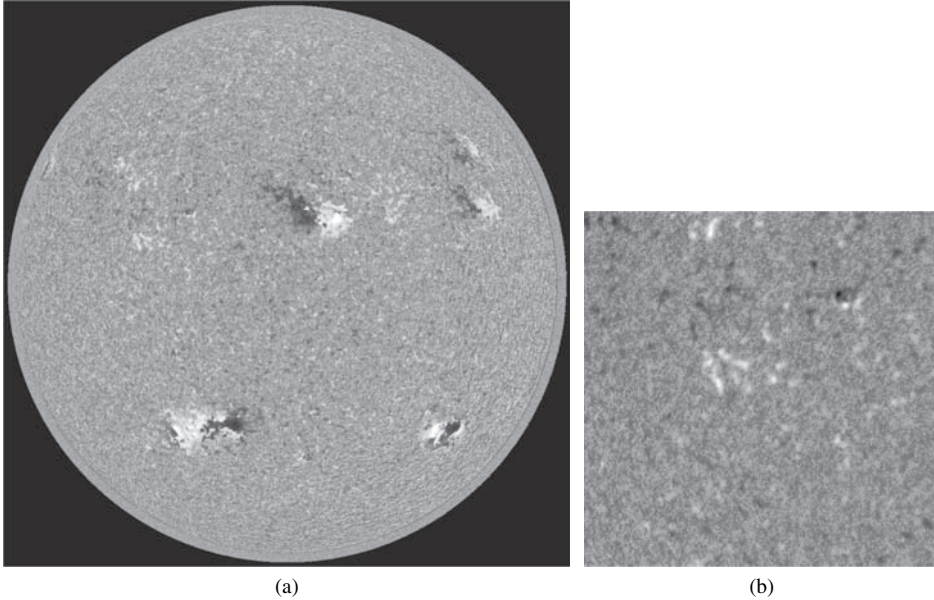
10   *The solar atmosphere*

(a)   (b)

Fig. 1.4. (*a*) Full Sun magnetogram from data obtained with the Michelson Doppler Imager on *SOHO* on 1997 September 11. Black areas indicate negative line-of-sight field concentrations; white areas positive line-of-sight field concentrations. A number of major active regions are evident, with concentrations of opposite field close to each other. (*b*) A portion of this magnetogram in the eastern part of the Sun, measuring 250×250 pixel^2, devoid of active regions but showing a mixture of positive and negative polarities. These are field concentrations at supergranule boundaries, and are present all over the Sun's surface away from active regions. The pixel size is 1 arcsecond, or 725 km. In both images (as in nearly all solar images in this book), north is at the top, east to the left. Courtesy the *SOHO* MDI Team.

supergranular cell boundaries, so appearing as a honeycomb structure over the whole Sun. It shows most clearly at the apparent centre of the Sun's disk as seen from Earth.

The network is especially prominent when viewed at the wavelengths of ultraviolet emission lines that are formed in the upper chromosphere (10^4 K) or at transition region temperatures ($\sim 10^5$ K), i.e. at greater altitudes above the photosphere than the Hα or Ca II H and K lines (see Figure 1.1). Thus, in the chromospherically formed emission lines of neutral helium (He I), e.g. the resonance line at 584 Å, the network over the entire Sun gives rise to a mottled appearance to the Sun, like the surface of an orange. This is illustrated by full Sun ultraviolet images from the SUMER instrument on the *SOHO* spacecraft (Figure 1.5). The He I resonance line is formed in the upper chromosphere, where the temperature is about 20000 K. The network has much the same nature at higher temperatures, 10^5 K, characteristic of the transition region.

With imaging spectrometers, such as the Coronal Diagnostic Spectrometer (CDS) on the *SOHO* spacecraft, the network can be traced at different temperatures forming images in extreme ultraviolet emission lines of ions having a large variety of characteristic temperatures. This is illustrated in Figure 1.6, where images in chromospheric lines (He I, He II), transition region lines (O III, O IV, O V, Ne VI), and coronal lines (Mg VIII, Mg IX, Mg X, Si VIII) are